Supplementary Information for

Theoretical determination of superior high-temperature thermoelectricity in the n-type doped 2H-ZrI_2 monolayer

Jia Wen, Jie Peng, Bokai Zhang, and Zhi-Yong Wang*

School of Physical Science and Technology,

Southwest University, Chongqing 400715, China and

Chongqing Key Laboratory of Micro-Nano Structure Optoelectronics, Chongqing 400715, China

* Corresponding author: zywang@swu.edu.cn (Z.-Y. Wang).

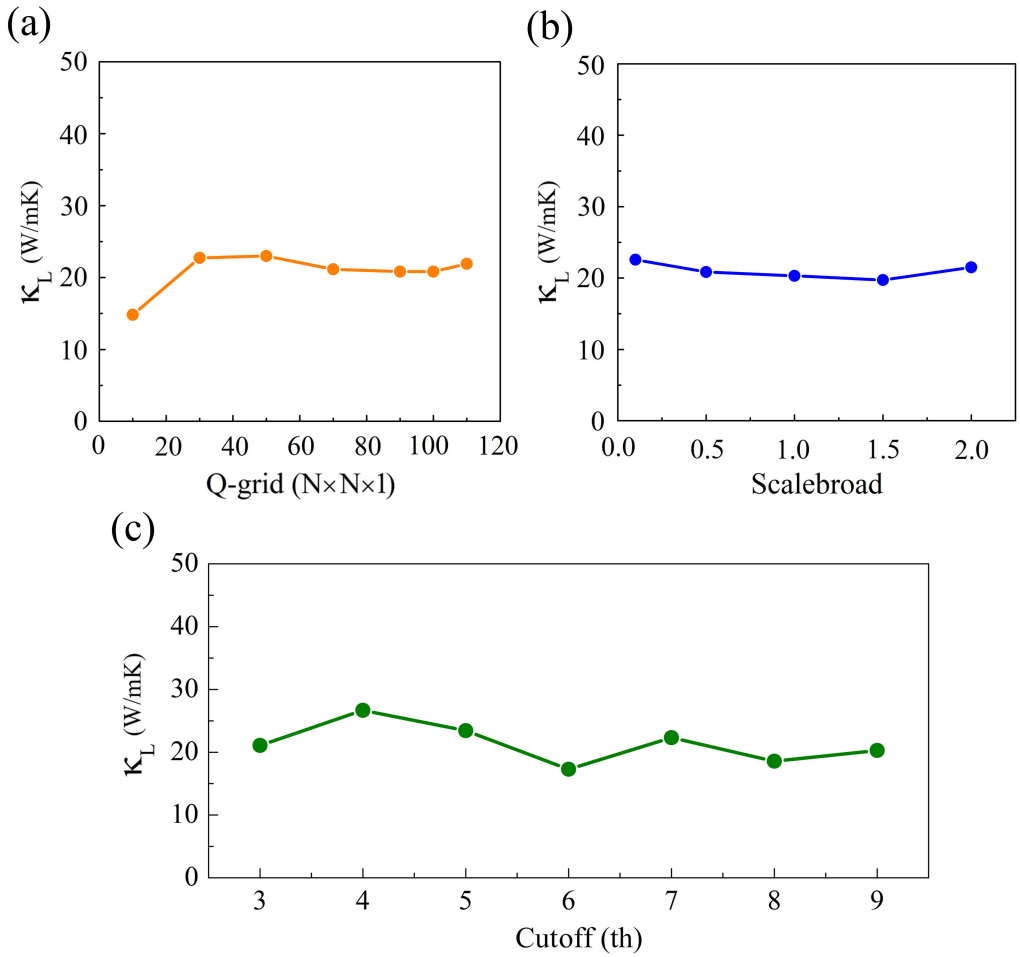

Fig. S1: Convergence test data of the thermal conductivity with respect to (a) the **k**-point mesh size, (b) the scalebroad parameter, and (c) the nearest neighbors. It is clear that the convergent result can be realized at scalebroad = 1.0. After a series of test calculations, we choose a 100 × 100 × 1 **k**-point mesh and the interaction cutoff of 9 nearest neighbors for the third-order IFCs to calculate the thermal conductivity of monolayer ZrI_2 at different temperatures.

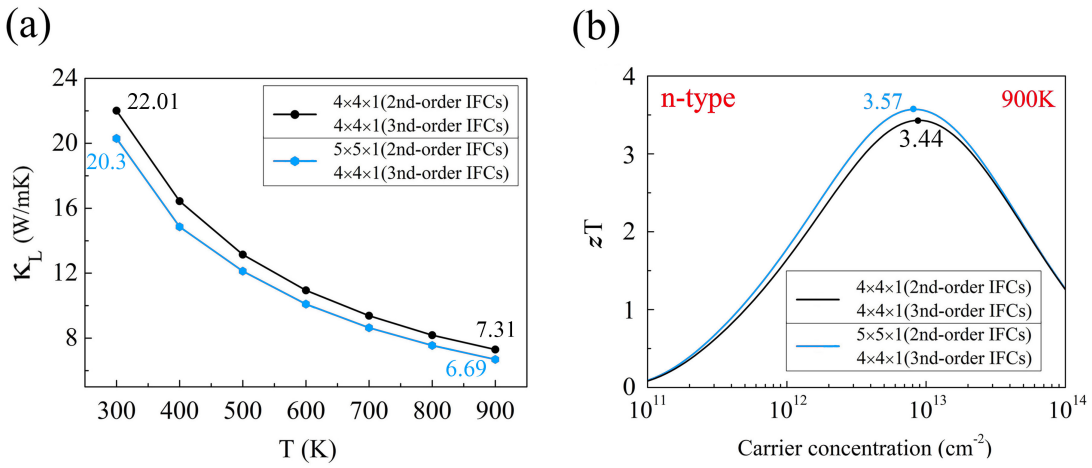

Fig. S2: (a) Impact of supercell size inconsistency in the calculations of the second-order and third-order IFCs on the lattice thermal conductivity and (b) resultant slightly overestimated optimal figure of merit from 3.44 to 3.57 for n-type doped ZrI_2 monolayer at 900 K.

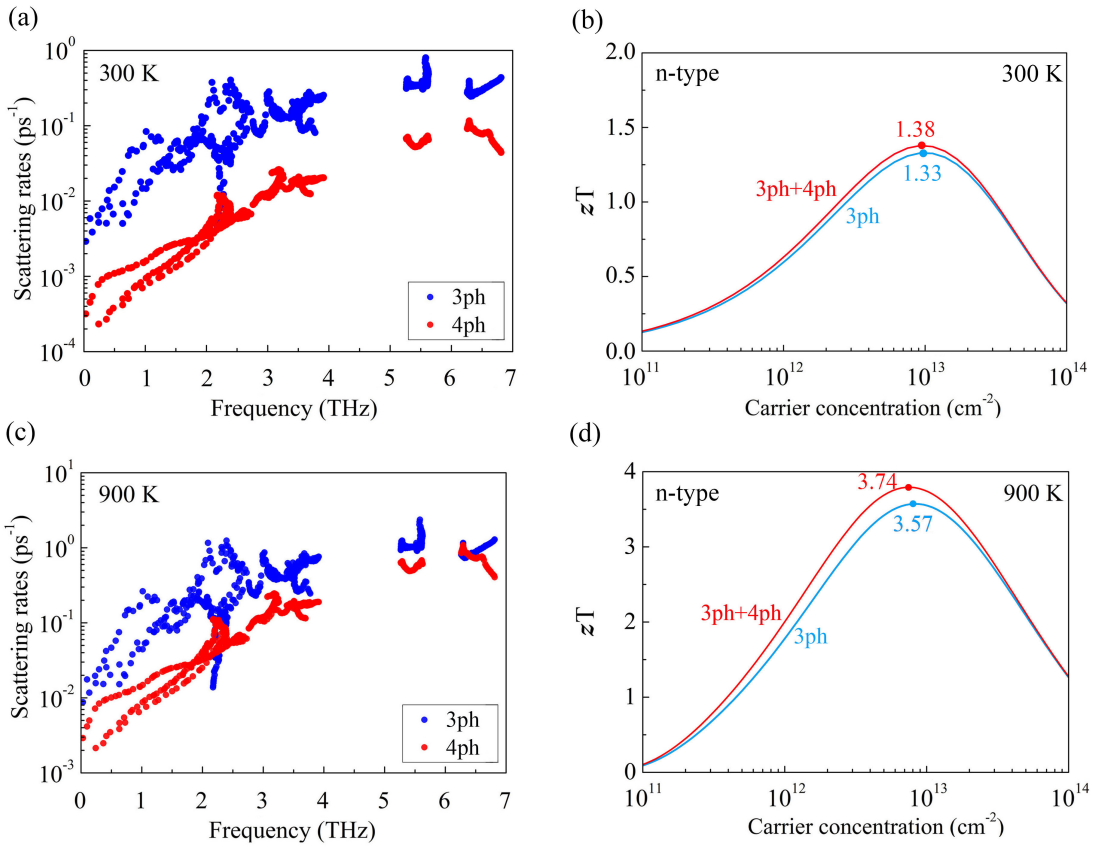

Fig. S3: Phonon scattering rates and n-type figure of merit of monolayer ZrI_2 at 300 and 900 K. It is clear that four-phonon (4ph) scattering rates are remarkably less than three-phonon (3ph) scattering rates over the entire frequency range, implying that the former can be simply treated as a high-order perturbation. To be specific, the lattice thermal conductivity after including 4ph scattering is calculated to be 19.12/5.77 W m^{-1} K^{-1} at 300/900 K, resulting in a slightly overestimated optimal figure of merit from 1.33/3.57 to 1.38/3.74 for n-type doped ZrI_2 monolayer. Note that in both case, a $4 \times 4 \times 1$ supercell with a $30 \times 30 \times 1$ **k**-point mesh is considered to calculate the anharmonic four-order IFCs up to the 4th-nearest neighbors by the Fourthorder.py script.[1]

Table S1: Calculated in-plane stiffness (B_{2D}), shear modulus (G_{2D}), mean sound velocity (v_m), Debye temperature (Θ), and Grüneisen parameter (γ_e) from isotropic approximation for the ZrI_2 monolayer.

Material	B_{2D} (N m^{-1})	G_{2D} (N m^{-1})	v_m (km s^{-1})	Θ (K)	γ_e
ZrI_2	36.53	26.27	2.64	349.87	1.15

According to the elastic constants from the energy-strain scheme,[2] the in-plane stiffness (B_{2D}), the shear modulus (G_{2D}), and the Poisson's ratio (ν) can be obtained by the following formulas[3–6]

$$B_{2D} = \frac{C_{11} + C_{12}}{2},\ G_{2D} = C_{44}, \text{and } \nu = \frac{C_{12}}{C_{11}}, \tag{S1}$$

which are then employed to calculate the sound velocities of the TA and LA branches

$$v_{LA} = \sqrt{\frac{B_{2D} + G_{2D}}{\rho_{2D}}} \tag{S2}$$

and

$$v_{TA} = \sqrt{\frac{G_{2D}}{\rho_{2D}}}, \tag{S3}$$

where ρ_{2D} corresponds to the 2D mass density equal to $4.53 \times 10^{-3} g$ m^{-2} for monolayer ZrI_2. The mean sound velocity can be written as

$$v_m = \left[\frac{1}{3}\left(\frac{1}{v_{LA}^3} + \frac{2}{v_{TA}^3}\right)\right]^{-1/3}. \tag{S4}$$

The Debye temperature can be computed from the mean sound velocity

$$\Theta = \frac{\hbar v_m}{k_B}\left(\frac{4\pi N}{S}\right)^{1/2}, \tag{S5}$$

where $\hbar$, k_B, N, and S are the reduced Planck constant, the Boltzmann constant, the number of atoms in the unit cell, and the area of the unit cell, respectively. Finally, we can obtain Grüneisen parameter from the Poisson's ratio

$$\gamma_e = \frac{3}{2}\left(\frac{1+\nu}{2-3\nu}\right). \tag{S6}$$

As shown in Table S1, the calculated Debye temperature reaches up to 349.87 K on the one hand, and the Grüneisen parameter is calculated to be as low as 1.15 on the other hand. According to Slack's theory,[7] the high Debye temperature implies a high lattice thermal conductivity. This is because a higher Debye temperature indicates that a larger number of phonon modes are frozen out, thus giving rise to a decrease in the phonon scattering rates. Similarly, the small Grüneisen parameter manifests a weak anharmonicity, suppressing the strength of phonon scattering, which in turn enlarges the lattice thermal conductivity as well.

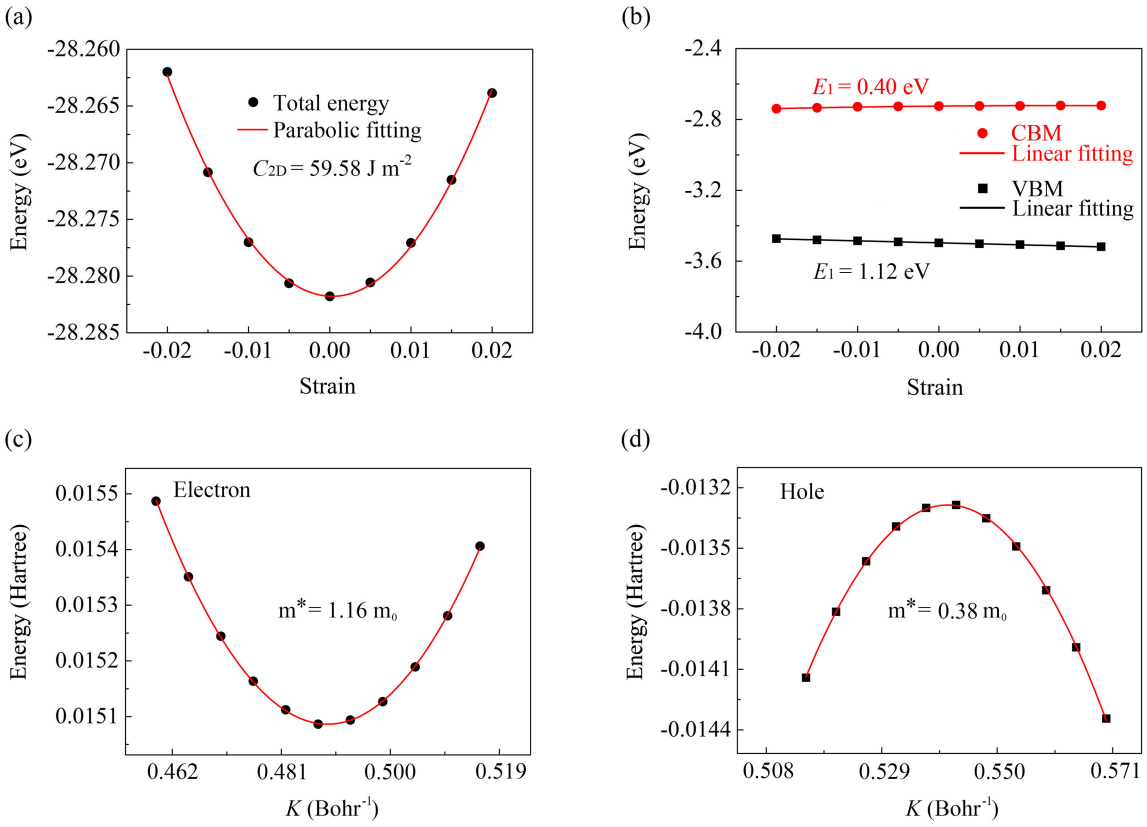

Fig. S4: (a) Total energy and (b) shift of band edges for monolayer ZrI_2 with respect to uniaxial strain along the zigzag direction. The elastic modulus can be obtained via the quadratic fitting of total energy, and the DP constant via the linear fitting of band edges. The effective masses of (c) electrons and (d) holes for monolayer ZrI_2, which can be fitted respectively by the energy of **k** states in the first Brillouin zone around the conduction band minimum and valence band maximum with parabolic curves for the zigzag direction.

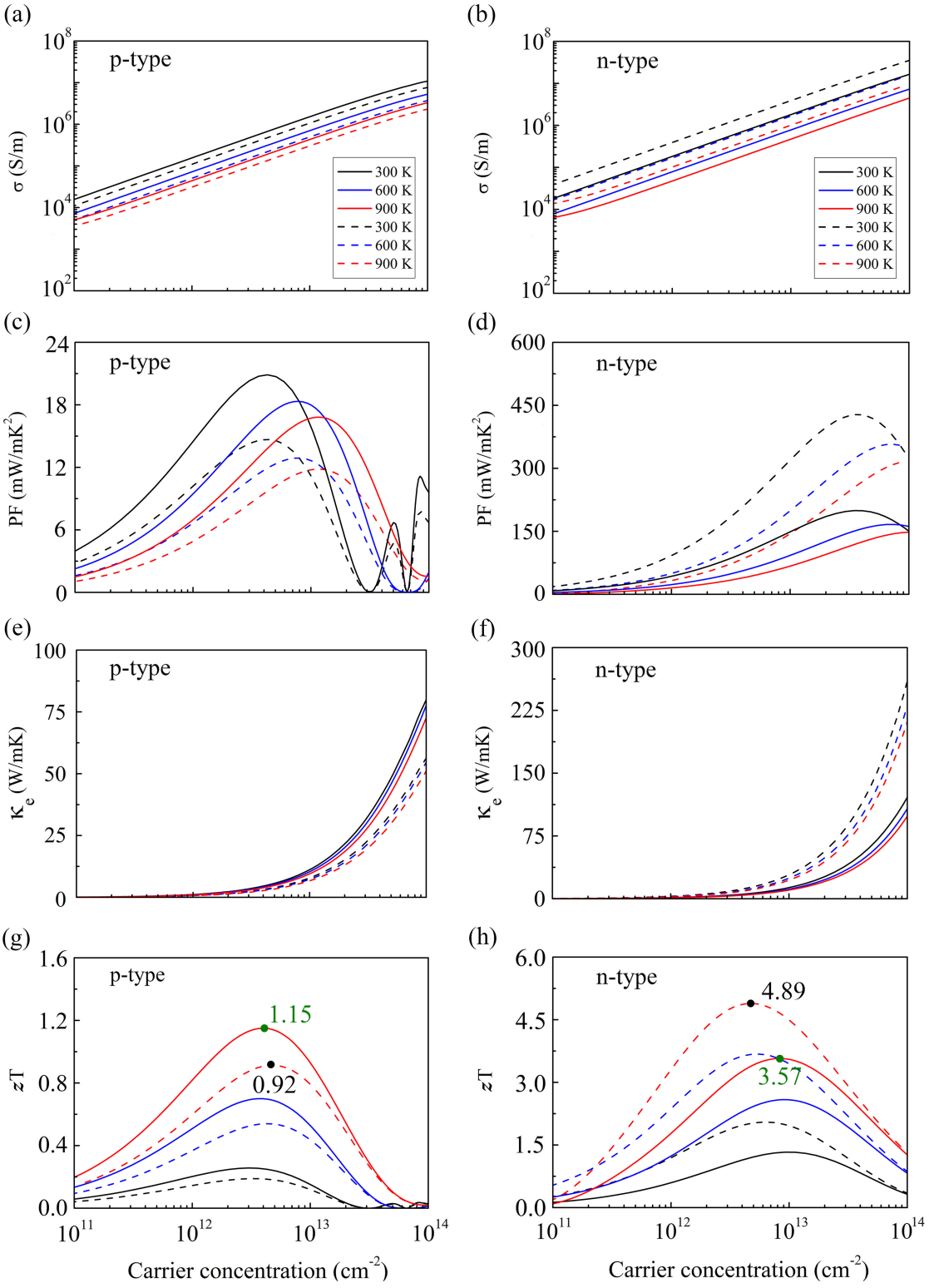

Fig. S5: Electrical conductivity, power factor, electronic thermal conductivity, and figure of merit for p-type and n-type doped ZrI_2 monolayers at different temperatures as a function of carrier concentration. The solid and dashed curves are based on the different carrier relaxation time by Eq. (3) and Eq. (S7), respectively.

Table S2: Calculated elastic modulus (C_{2D}), DP constant (E_1), carrier effective mass (m^*_{M-K} and $m^*_{\Gamma-M}$), and carrier relaxation time (τ) of the ZrI_2 monolayer at room temperature. Note that m_0 denotes the mass of a free electron.

Carrier type	C_{2D} (J m^{-2})	E_1 (eV)	m^*_{M-K} (m_0)	$m^*_{\Gamma-M}$ (m_0)	τ ($\times 10^{-13}$ s)
Electron	59.58	0.40	0.63	1.06	55.83
Hole	59.58	1.12	0.38	1.72	7.12

Apart from Eq. (3) in the main text, we recalculate the carrier relaxation time by deformation potential theory with another alternative expression[8,9]

$$\tau = \frac{\hbar^3 C_{2D}}{k_B T m_d E_1^2}, \tag{S7}$$

where $\hbar$, C_{2D}, k_B, T, m_d, and E_l are the reduced Planck constant, 2D elastic modulus, Boltzmann constant, absolute temperature, mean effective mass, and DP constant, respectively, and the mean effective mass is determined by $m_d = \sqrt{m^*_{\Gamma-M} m^*_{M-K}}$. Table S2 lists all calculated parameters of monolayer ZrI_2 subject to Eq. (S7) at room temperature. At the same time, Fig. S5 displays the corresponding electrical conductivity, power factor, electronic thermal conductivity, and figure of merit for p-type and n-type doped ZrI_2 monolayers at different temperatures and varying carrier concentrations. For comparison, all electronic transport quantities of interest constrained to the Eq. (3) are presented as well in Fig. S5 under the same conditions. As seen, the introduction of Eq. (S7) overestimates the figure of merit of n-type doped ZrI_2 monolayers. For example, the optimal figure of merit is significantly increased from 3.57 to 4.89 at 900 K. On the contrary, the figure of merit is underestimated for p-type doped ZrI_2 monolayers.

[1] Z. Han, X. Yang, W. Li, T. Feng and X. Ruan, *Comput. Phys. Commun.*, 2022, **270**, 108179.

[2] E. Cadelano and L. Colombo, *Phys. Rev. B: Condens. Matter Mater. Phys.*, 2012, **85**, 245434.

[3] E. Bolen, E. Deligoz and H. Ozisik, *Solid State Commun.*, 2021, **327**, 114223.

[4] B. Peng, H. Zhang, H. Shao, Y. Xu, G. Ni, R. Zhang and H. Zhu, *Phys. Rev. B: Condens. Matter Mater. Phys.*, 2016, **94**, 245420.

[5] A. Politano and G. Chiarello, *Nano Res.*, 2015, **8**, 1847-1856.

[6] H. H. Huang, X. Fan, D. J. Singh and W. T. Zheng, *J. Mater. Chem. C*, 2020, **8**, 9763-9774.

[7] G. A. Slack, *J. Phys. Chem. Solids*, 1973, **34**, 321-335.

[8] J. Qiao, X. Kong, Z.-X. Hu, F. Yang and W. Ji, *Nat. Commun.*, 2014, **5**, 4475.

[9] Y. Wang, Z. Gao and J. Zhou, *Physica E*, 2019, **108**, 53-59.